Published in final edited form as:
Chemistry. 2014 July 14; 20(29): 8842–8847. doi:10.1002/chem.201403027.

Supramolecularly-knitted Tethered Oligopeptide/Single-walled Carbon Nanotube Organogels

Dr. Jiong Zou, **Xun He**, **Jingwei Fan**, **Dr. Jeffery E. Raymond**, and **Dr. Prof. Karen L. Wooley**
Departments of Chemistry and Chemical Engineering, Laboratory for Synthetic-Biologic Interactions, Texas A&M University, P.O. BOX 30012, 3255 TAMU, College Station, TX 77842 (USA)

Karen L. Wooley: wooley@chem.tamu.edu

Abstract

A facile polymerization of an allyl-functional *N*-carboxyanhydride (NCA) monomer is utilized to construct an A-B-A type triblock structure containing β-sheet-rich oligomeric peptide segments tethered by a poly(ethylene oxide) chain, which are capable of dispersing and gelating single-walled carbon nanotubes (SWCNTs) noncovalently in organic solvents, resulting in significant enhancement of the mechanical properties of polypeptide-based organogels.

Keywords

carbon nanotube; oligopeptide; organogel; supramolecular assembly; ring opening polymerization

Since being synthesized in the early 1990s,[1] carbon nanotubes (CNTs) have drawn significant interest due to their extraordinary optical, thermal, mechanical and electronic properties.[2] Single-walled carbon nanotubes (SWCNTs) are particularly intriguing, typified as one-atom-thick graphite lattices rolled into cylindrical nanostructures with a diameter range of 0.4–3 nm and varying chirality. SWCNTs have been extensively explored for a variety of applications, such as optical emitting devices,[3] flame-retardant coatings,[4] mechanical reinforcing materials,[5] flexible electronics,[6] sensors[7] and many others.[8] Recently, increasing attention has been given to the incorporation of SWCNTs in biological systems to take advantage of their near-infrared (NIR) responsive exothermicity properties[9] in drug delivery,[10] tissue engineering,[11] cancer diagnoses and therapy,[12] among other applications.

However, due to the extremely strong π-π stacking and van der Waals interactions, large SWCNT bundles tend to be difficult to disperse homogeneously in common organic and aqueous solutions. This challenge imposes significant limitations on the use of SWCNTs after they have aggregated. With the help of prolonged sonication, SWCNTs can be dispersed in some solvents, though precipitation occurs soon thereafter.[13] Two common approaches applied to this dispersion problem include covalent modification of SWCNT

Correspondence to: Karen L. Wooley, wooley@chem.tamu.edu.
Supporting information for this article is available on the WWW under http://www.chemeurj.org/ or from the author.

surfaces and noncovalent adsorption of functional small molecules and polymers.[14] Noncovalent modification of SWCNTs is particularly attractive because the strategy preserves the intrinsic properties of SWCNTs without disruption to the electronic and optical responses of the system.[15] It has been demonstrated that SWCNTs interact with conjugated species, such as pyrene derivates,[16] phthalocyanines,[17] porphyrins,[18] phenazine,[19] and thionine types of dyes,[20] based on π-π stacking. Twelve-membered cyclodextrins[21] and select DNA sequences[22] have also been reported to allow structure-specific recognition of SWCNTs with specific surface structure due to host-guest supramolecular complexation. Compared with small molecule SWCNT stabilizers, functional polymers are quite efficient dispersants, due to an ability to wrap around SWCNTs, thereby, displacing and disrupting the van der Waals and π-π interactions between aggregated SWCNTs. Different polymeric systems, including acrylates,[23] epoxy resins,[24] hydrocarbon polymers[8b] and conjugated polymers,[25] have been developed for CNT dispersal in organic solvents. However, limited studies have been conducted using biodegradable polymers to disperse CNTs.[22, 26]

Polypeptides with tunable sequences and secondary structures have been employed to noncovalently disperse CNTs in aqueous solutions.[27] By tuning the sequence and length of these polypeptide systems, differentiated binding affinity for different types of SWCNTs could be realized.[28] Specifically, the secondary structure (α-helix[27b, 29] and β-sheet[30] formation) of an intelligently-designed amphiphilic polypeptide system was reported to bind the surface of SWCNTs in aqueous solutions. However, the polypeptide-SWCNT dispersal remained primarily limited to sequences composed of 12–30 natural amino acids, with π-π stacking between aromatic residues (derived from amino acids such as tyrosine, phenylalanine and histidine) on polypeptide and the SWCNT surface playing the most important role in the polypeptide dispersing capability. The dispersion of SWCNTs by nonaromatic peptides has not been reported. Typically, the synthesis of polypeptide dispersants with special sequences has required several steps of solid phase synthesis and has experienced technical challenges with production scale-up.[31] Compared with solid phase synthesis, ring opening polymerization (ROP) of *N*-carboxyanhydrides (NCA) provides a more effective, scalable and economic method for the preparation of high molecular weight polypeptides for SWCNT dispersion.[26d]

Recently, our group reported a functional polypeptide-based organogelator, poly(ethylene oxide)-*block*-poly(DL-allylglycine) (PEO-*b*-PDLAG), containing a racemic allyl functional homopolypeptide block.[32] Gelation in high polar organic solvents was shown to be driven by supramolecular assembly of the PDLAG peptide segment into β-sheets. With β-sheet formation, hierarchical one-dimensional stacking of block copolymers then led to the construction of well-defined ribbon-like morphologies and, ultimately, gelation. The present work stems from the hypothesis that β-sheets composed of allyl-rich PDLAG peptide domains would have a strong propensity for π-π stacking with SWCNT surfaces.

It was anticipated that the diblock PEO-*b*-PDLAG would lead merely to dispersion of SWCNT, whereas our interest in this work was the creation of functional hybrid organogels reinforced by SWCNTs. Therefore, a new triblock cooligopeptide oligo(DL-allylglycine)-*block*-poly(ethylene oxide)-*block*-oligo(DL-allylglycine) (ODLAG-*b*-PEO-*b*-ODLAG) was

designed to allow for binding to and bridging between SWCNTs. The ODLAG peptide β-sheets are shown to undergo noncovalent association with the SWCNTs, while also regulating assembly into hierarchically-ordered structures *via* peptide-peptide interactions between adjacent ODLAG-*b*-PEO-*b*-ODLAG-decorated SWCNTs. The triblock structure formed β-sheets and showed good ability to homogeneously disperse SWCNTs in DMF solution. With increased polymer concentration, the triblock-SWCNT composites resulted in fibrillar organogels. Compared with the ODLAG-*b*-PEO-*b*-ODLAG organogel without SWCNTs, the triblock-SWCNT composite organogels possess significantly increased stiffness as characterized by dynamic mechanical analysis (DMA). The triblock-SWCNT organogels were characterized at different length scales including scanning electron microscopy (SEM), transmission electron microscopy (TEM), confocal microscopy and atomic force microscopy (AFM). Interestingly, with disruption of the β-sheeting, the triblock could no longer disperse SWCNTs or form organogels. Based upon the hypothesis and results, this work has demonstrated a new and efficient strategy to disperse SWCNTs.

With our broad interest in the creation of original well-defined functional polymer-based nanomaterials having simple molecular design and synthetic feasibility, for fundamental studies and biomedical applications, we began investigation into the preparation of A-B-A type amphiphilic triblock copolypeptides having broadly modifiable allyl side chains. Shvartzman-Cohen *et al.* reported an amphiphilic A-B-A type triblock copolymer, poly(ethylene oxide)$_{100}$-*b*-poly(propylene oxide)$_{65}$-*b*-poly(ethylene oxide)$_{100}$, (PEO$_{100}$-*b*-PPO$_{65}$-*b*-PEO$_{100}$) as an efficient SWCNT disperser in aqueous solution *via* noncovalent interaction between polymers and SWCNT surfaces, and further shaped the inter-nanotube potential against aggregation.[33] We had expected that a triblock structure having an inversion of the positioning of the amphiphilic units, to a structure with peptide-based hydrophobic end blocks capable of binding to the surface of hydrophobic SWCNT and tethered by a central polar segment could disperse SWCNT in polar solvents and, further, lead to gelation properties. A ODLAG-*b*-PEO-*b*-ODLAG triblock structure **1** was, therefore, synthesized *via* facile ring opening polymerization of DL-allylglycine NCA by using α,ω–diamino terminated poly(ethylene oxide) (NH$_2$-PEO$_{68}$-NH$_2$) as the macroinitiator (Scheme 1). Our recent study found that by using normal Schlenk techniques, NCA ROPs can be conducted on a large scale with the rate of polymerization being controlled by a straightforward nitrogen flow method.[34] For the current investigation, the required amounts of allyl functional NCA monomers and diamino macroinitiator were dissolved in anhydrous DMF and the ROP was allowed to proceed up to 12 h at room temperature, under a continuous nitrogen flow (flow rate = 100 mL/min). The conversion of the monomer was monitored by measuring the intensity of the DLAG NCA anhydride peak at 1788 cm^{-1} using attenuated total reflectance-Fourier transform infrared spectroscopy (ATR-FTIR). After monomer conversion of > 95% was obtained, the polymerization was quenched by pouring the viscous reaction mixture into diethyl ether and dried under vacuum to yield the targeted triblock structure as a white powder. Similar to previously reported DLAG NCA polymerization, the A-B-A triblock had a tendency to form a gel in DMF at high conversion. The detailed structures, compositions and thermal properties of the triblock structures were determined by using ^{1}H NMR, ^{13}C NMR, ATR-FTIR, DSC and TGA analyses (see SI). The processing capability of **1** was explored in terms of secondary structures, supramolecular

interaction with SWCNTs, gelation behavior and mechanical properties of organogels with/without SWCNTs incorporated. The capability of **1** to form organogels in different solvents was explored and the properties of the gels in DMF were investigated comprehensively (Table S1). The triblock structure could be dissolved in polar organic solvents (DMF, DMSO, methanol, TFA and chloroform), but not in apolar organic solvents or water, indicating that the solvation properties were dominated by the oligopeptide end block properties. With an increase in concentration (up to 50 mg/mL) the **1** DMF solution tended to form organogels (r.t., 1~5 h). Gelation was driven by supramolecular assembly of β-sheets into well-defined fiber-like nanostructures, further generating a 3-D networks through longer-range interactions. This result is similar to that observed for the $mPEO_{45}$-*b*-$ODLAG_{12}$ diblock copolymer organogelators reported previously. The triblock **1** DMF organogel also responded to sonication stimulus, rapidly obtaining a sol state (20 s sonication). SWCNTs (0.5 mg/mL) incorporated into solutions of **1** (50 mg/mL) formed homogeneous SWCNT DMF solutions (2 min sonication). After standing (r.t., 5 h), self-supported uniform SWCNTs DMF gels formed. It was also found that the ability of **1** to undergo dispersion and gelation with SWCNTs changed with different organic solvents (Table S1). Compared with DMF, similar SWCNT loading into DMSO or methanol solutions resulted in SWCNT precipitates that did not gel with time (r.t., 24 h). The critical gel concentrations (CGCs, Table S2) were obtained by preparing different polymer concentrations in DMF, DMSO and methanol (test tube inversion method, r.t.), with DMF requiring the lowest concentration for gelation. With the incorporation of SWCNTs, the CGC of **1** in DMF increased from 10 mg/mL to 25 mg/mL, while the CGC in DMSO was not observed even at 100 mg/mL. The increase of CGC after SWCNT incorporation indicates strong noncovalent interaction between the SWCNTs and oligopeptide segments, resulting in a decrease in available peptide-peptide interactions. However, while TFA was used as solvent, **1** could be totally dissolved unimolecularly by disrupting the supramolecular secondary structure. The SWCNT could not be homogeneously suspended in TFA solutions of **1**, which indicated that the β-sheeting is a critical component of both gelation and SWCNT dispersion.

The dispersion ability of SWCNTs by $ODLAG_6$-*b*-PEO_{68}-*b*-$ODLAG_6$ was characterized by using UV-vis spectroscopy. SWCNT (0.20 mg) was suspended into DMF (1 mL, r.t., 2 min sonication) resulting in SWCNT precipitation within 2 min after sonication (Figure 1b). In comparison, **1** (5 mg) was added to a similar SWCNT DMF suspension (1 mL, at 0.2 mg/mL, 2 min sonication) and a homogeneous SWCNT dispersion was obtained. The solution was stable (1 week in r.t.) and no precipitation was observed. UV-vis absorbance spectra were measured after five-fold dilution of the **1**-SWCNT DMF solution. As a control, the $ODLAG_6$-PEO_{68}-$ODLAG_6$ in DMF (1 mg/mL) showed very low absorbance in UV-Vis. In the absorbance spectrum of **1**-SWCNT composites, the second interband transitions (S_{22}) for semiconducting SWCNTs can be found from 600–800 nm, and the absorption band around 550 nm can be assign to the first interband transitions (M_{11}) of metallic SWCNTs. The dispersion ability of NH_2-PEO_{68}-NH_2 was also measured at the concentration of 1 mg/mL, indicating that without the aid of the oligopeptide segments, the PEO block could not disperse SWCNTs in DMF.

The nanoscopic supramolecular self-assembly of **1**-SWCNTs composites was characterized by TEM (Figure 2a and Figure S1). SWCNTs interacting with the triblock structures exhibited higher contrast and increased diameter (*ca*. 6.4 nm, Figure 2a) when compared with the SWCNT without oligopeptide association (*ca.* 3.2 nm, Figure 2b). Upon interaction with **1**, the bent SWCNT fibers exhibited much more flexible morphology and had a tendency to form quasi-aligned aggregates. Hierarchical nanoscopic structures could also be observed in the **1**-SWCNT composites (Figure 3c). "Knitted" fibers, have spacing between SWCNTs that indicate several polymers associating and encapsulating, further reinforce the function of the β-sheets as both SWCNT binding and self-binding. The allyl-rich segments in the triblock nanoribbon may also serve as conjugation-rich domains which interact with the sidewalls of SWCNTs resulting in both plaquing (β-sheets driven) and π-π stacking effects contributing to the triblock SWCNT interactions. By observation (Figure S1) the **1** supramolecular fibril assemblies tend to take a helical conformation, wrapping around the SWCNTs, which suggests that a soluble PEO "shell" disperses the SWCNTs, and is in keeping with peptide driven polymer-SWCNT interactions. In contrast, control studies of the SWCNT or organogel, each independently, gave much less interesting features. A cylindrical morphology was observed in **1** DMF organogel with phosphotungstic acid (PTA) staining. The width of the cylinder was ~ 8.8 nm and the length ~ 100–300 nm (Figure 2c). Without PTA staining, the cylinders could only be observed sparingly by TEM imaging (Figure 2d). The gels were also characterized at the meso scale (SEM, AFM and confocal microscopy). Porous network structures could be observed in both SEM and AFM characterizations (Figures S2–S3). Dye doping of the **1** and **1**-SWCNT gels indicated a greater homogeneity within the gel on addition of the SWCNTs (confocal and fluorescence life-time imaging, Figures S7–S8).

Characterization by FT-IR spectroscopy was conducted to investigate the secondary structure and the binding between **1** and SWCNTs (Figure 3 and S4). Signatures of the β-sheet secondary structure for **1** were observed at 1670 cm^{-1} and 1620 cm^{-1} (both in amide I), in combination with a peak at 1520 cm^{-1} (amide II). The spectra of **1** and **1**-SWCNT composites were almost identical, as the SWCNT did not present peaks in these frequency ranges, which suggests that the supramolecular structure of the oligopeptide gelator was unperturbed[35] by the SWCNTs. Raman spectroscopy measurements also indicated that the triblock structure could disperse SWCNTs in DMF solutions as well as in DMF gels without changing the structure of the SWCNTs (Figure S5). The D band ~1300 cm^{-1} and G band ~1600 cm^{-1} of **1**-SWCNT gels and **1**-SWCNT solutions are almost identical to the pristine SWCNT in a DMF suspension. Compared with the SWCNT DMF suspension, the significantly increased G-band intensity with respect to the D-band intensity in the **1**-SWCNT gel indicates a decrease in disruption of π-rich lattice (SWCNT-SWCNT interactions), further confirming the dispersive capability of the oligopeptide triblock.

The thermogravimetric analyses (TGA) were conducted to measure the mass loss of **1**-SWCNT composites, **1** and SWCNT (Figure 4). The **1**-SWCNT composites exhibited two decompositions at 300–400 °C and at 400–650 °C, which can be attributed to the decomposition of **1** (75.2% mass loss at 300–425 °C) and SWCNTs (84.1% mass loss at 400–660 °C), respectively.

The mechanical properties of **1**-SWCNT DMF gels were characterized by DMA. With 1.5 wt% incorporation of SWCNTs, the **1**-SWCNT composites DMF gel (50 mg/mL) had a storage modulus ~400 kPa, (Figure S6) which is >2 orders-of-magnitude greater than the **1** gel without SWCNT. The **1** DMF gel with same concentration (50 mg/mL) was too soft to be measured by DMA (storage modulus < 1 kPa). Given the evidence for high dispersion of SWCNTs in this system, this result was expected as the SWCNTs provide reinforcement to the gel network through exceptionally strong SWCNT-polymer binding.

In conclusion, single-walled carbon nanotubes were efficiently dispersed in a novel A-B-A type triblock network, with low compositional and structural complexity, being based upon a hydrophilic PEO middle block and two hydrophobic racemic synthetic oligopeptide end segments. Detailed characterization studies indicated that the supramolecular self-assembly of β-sheets in the oligopeptide blocks form one dimensional stacked nanoribbons, in which allyl-rich ODLAG peptide domains have strong propensity for π-π stacking with SWCNT surfaces, and consequently, efficiently separated and dispersed SWCNTs in organic solvent. The ODLAG peptide β-sheets could both noncovalently associate with the SWCNTs and assemble peptide-coated nanotubes into hierarchically-ordered structures *via* peptide-peptide interactions. Despite these structures manifesting on the nanoscale, micro/mesoscale homogeneity was increased in the composite gels when compared to the triblock gel alone. With the incorporation of SWCNTs the mechanical properties of triblock-based organogels increased greatly, further displaying a dispersed (not merely encapsulated) state in the gel matrix. This work provides an interesting strategy that uses secondary structure control to stabilize SWCNTs, allowing for the efficient noncovalent incorporation of SWCNTs in the polymeric matrix without disrupting the band-structure of the SWCNTs (Raman). Moreover, sonication-responsive properties, enhanced mechanical properties and the presence of known biodegradable moieties enable further study and potential applications in sensor design, construction of adaptive materials and controlled release systems.

Acknowledgments

This work was supported in part from the National Heart Lung and Blood Institute of the National Institutes of Health as a Program of Excellence in Nanotechnology (HHSN268201000046C) and the National Science Foundation under grant number DMR-1105304. The Welch Foundation was gratefully acknowledged for support through the W. T. Doherty-Welch Chair in Chemistry, Grant no. A-0001. The microscopy & imaging center (MIC) at Texas A&M University was also gratefully acknowledged.

References

1. Iijima S. Nature. 1991; 354:56–58.
2. a) Shulaker MM, Hills G, Patil N, Wei H, Chen H-Y, PhilipWong H-S, Mitra S. Nature. 2013; 501:526–530. [PubMed: 24067711] b) Subramaniam C, Yamada T, Kobashi K, Sekiguchi A, Futaba DN, Yumura M, Hata K. Nat Commun. 2013:4.c) Franklin AD, Luisier M, Han SJ, Tulevski G, Breslin CM, Gignac L, Lundstrom MS, Haensch W. Nano Lett. 2012; 12:758–762. [PubMed: 22260387] d) Brunetti FG, Romero-Nieto C, López-Andarias J, Atienza C, López JL, Guldi DM, Martín N. Angew Chem Int Ed. 2013; 52:2180–2184.
3. Yang L, Wang S, Zeng Q, Zhang Z, Peng LM. Small. 2013; 9:1225–1236. [PubMed: 23529815]
4. Liu Y, Wang X, Qi K, Xin JH. J Mater Chem. 2008; 18:3454–3460.
5. Chen T, Wang S, Yang Z, Feng Q, Sun X, Li L, Wang ZS, Peng H. Angew Chem Int Ed. 2011; 50:1815–1819.

6. Peng H. J Am Chem Soc. 2008; 130:42–43. [PubMed: 18072781]
7. Peng H, Sun X, Cai F, Chen X, Zhu Y, Liao G, Chen D, Li Q, Lu Y, Zhu Y, Jia Q. Nat Nanotechnol. 2009; 4:738–741. [PubMed: 19893530]
8. a) Calvaresi M, Zerbetto F. Acc Chem Res. 2013; 46:2454–2463. [PubMed: 23826731] b) Yang Y, Gupta MC. Nano Lett. 2005; 5:2131–2134. [PubMed: 16277439]
9. Kam NWS, O'Connell M, Wisdom JA, Dai H. Proc Natl Acad Sci USA. 2005; 102:11600–11605. [PubMed: 16087878]
10. Liu Z, Chen K, Davis C, Sherlock S, Cao Q, Chen X, Dai H. Cancer Res. 2008; 68:6652–6660. [PubMed: 18701489]
11. Harrison BS, Atala A. Biomaterials. 2007; 28:344–353. [PubMed: 16934866]
12. Ji SR, Liu C, Zhang B, Yang F, Xu J, Long JA, Jin C, Fu DL, Ni QX, Yu XJ. Bba-Rev Cancer. 2010; 1806:29–35.
13. Yu H, Hermann S, Schulz SE, Gessner T, Dong Z, Li WJ. Chem Phys. 2012; 408:11–16.
14. a) Tasis D, Tagmatarchis N, Bianco A, Prato M. Chem Rev. 2006; 106:1105–1136. [PubMed: 16522018] b) Grossiord N, Loos J, Regev O, Koning CE. Chem Mater. 2006; 18:1089–1099.c) Hirsch A. Angew Chem Int Ed. 2002; 41:1853–1859.d) Lee JJ, Yamaguchi A, Alam MA, Yamamoto Y, Fukushima T, Kato K, Takata M, Fujita N, Aida T. Angew Chem Int Ed. 2012; 51:8490–8494.e) Fukushima T, Kosaka A, Ishimura Y, Yamamoto T, Takigawa T, Ishii N, Aida T. Science. 2003; 300:2072–2074. [PubMed: 12829776]
15. a) Tuncel D. Nanoscale. 2011; 3:3545–3554. [PubMed: 21796303] b) Groschel AH, Lobling TI, Petrov PD, Mullner M, Kuttner C, Wieberger F, Muller AHE. Angew Chem Int Ed. 2013; 52:3602–3606.
16. Chen RJ, Zhang Y, Wang D, Dai H. J Am Chem Soc. 2001; 123:3838–3839. [PubMed: 11457124]
17. Cao L, Chen HZ, Zhou HB, Zhu L, Sun JZ, Zhang XB, Xu JM, Wang M. Adv Mater. 2003; 15:909–913.
18. Sprafke JK, Stranks SD, Warner JH, Nicholas RJ, Anderson HL. Angew Chem Int Ed. 2011; 50:2313–2316.
19. Jain D, Saha A, Marti AA. Chem Commun. 2011; 47:2246–2248.
20. Li QW, Zhang J, Yan H, He MS, Liu ZF. Carbon. 2004; 42:287–291.
21. Dodziuk H, Ejchart A, Anczewski W, Ueda H, Krinichnaya E, Dolgonos G, Kutner W. Chem Commun. 2003:986–987.
22. Tu X, Manohar S, Jagota A, Zheng M. Nature. 2009; 460:250–253. [PubMed: 19587767]
23. Du F, Fischer JE, Winey KI. Journal of Polymer Science Part B: Polymer Physics. 2003; 41:3333–3338.
24. Jin L, Bower C, Zhou O. Appl Phys Lett. 1998; 73:1197–1199.
25. a) Rice NA, Adronov A. Macromolecules. 2013; 46:3850–3860.b) Srinivasan S, Babu SS, Praveen VK, Ajayaghosh A. Angew Chem Int Ed. 2008; 47:5746–5749.c) Liang S, Zhao Y, Adronov A. J Am Chem Soc. 2013; 136:970–977. [PubMed: 24369733] d) Olivier JH, Deria P, Park J, Kumbhar A, Andrian-Albescu M, Therien MJ. Angew Chem Int Ed. 2013; 52:13080–13085.
26. a) Ding W, Eitan A, Fisher FT, Chen X, Dikin DA, Andrews R, Brinson LC, Schadler LS, Ruoff RS. Nano Lett. 2003; 3:1593–1597.b) Sitharaman B, Shi X, Walboomers XF, Liao H, Cuijpers V, Wilson LJ, Mikos AG, Jansen JA. Bone. 2008; 43:362–370. [PubMed: 18541467] c) Montenegro J, Vázquez-Vázquez C, Kalinin A, Geckeler KE, Granja JR. J Am Chem Soc. 2014; 136:2484–2491. [PubMed: 24471492] d) Tang H, Zhang D. J Polym Sci Pol Chem. 2013; 51:4489–4497.
27. a) Arnold MS, Guler MO, Hersam MC, Stupp SI. Langmuir. 2005; 21:4705–4709. [PubMed: 16032892] b) Zorbas V, Ortiz-Acevedo A, Dalton AB, Yoshida MM, Dieckmann GR, Draper RK, Baughman RH, Jose-Yacaman M, Musselman IH. J Am Chem Soc. 2004; 126:7222–7227. [PubMed: 15186159]
28. Wang S, Humphreys ES, Chung SY, Delduco DF, Lustig SR, Wang H, Parker KN, Rizzo NW, Subramoney S, Chiang YM, Jagota A. Nat Mater. 2003; 2:196–200. [PubMed: 12612679]
29. Dieckmann GR, Dalton AB, Johnson PA, Razal J, Chen J, Giordano GM, Munoz E, Musselman IH, Baughman RH, Draper RK. J Am Chem Soc. 2003; 125:1770–1777. [PubMed: 12580602]
30. Jeong WJ, Lim YB. Macromol Biosci. 2012; 12:49–54. [PubMed: 21936057]

31. Cheng J, Deming TJ. Top Curr Chem. 2012; 310:1–26. [PubMed: 21647839]
32. Zou J, Zhang F, Chen Y, Raymond JE, Zhang S, Fan J, Zhu J, Li A, Seetho K, He X, Pochan DJ, Wooley KL. Soft Matter. 2013; 9:5951–5958.
33. Shvartzman-Cohen R, Nativ-Roth E, Baskaran E, Levi-Kalisman Y, Szleifer I, Yerushalmi-Rozen R. J Am Chem Soc. 2004; 126:14850–14857. [PubMed: 15535711]
34. a) Zou J, Fan J, He X, Zhang S, Wang H, Wooley KL. Macromolecules. 2013; 46:4223–4226. [PubMed: 23794753] b) Fan J, Zou J, He X, Zhang F, Zhang S, Raymond JE, Wooley KL. Chem Sci. 2014; 5:141–150.
35. Mandal SK, Kar T, Das PK. Chem Eur J. 2013; 19:12486–12496. [PubMed: 23881597]

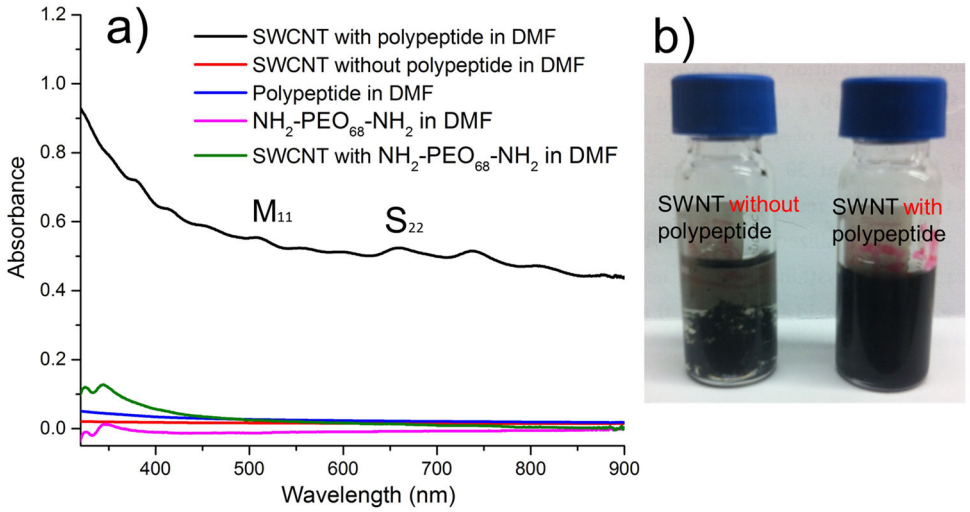

Figure 1.

a) UV-vis spectra of SWCNT in DMF with **1** (black); SWCNT in DMF with NH_2-PEO_{68}-NH_2 (green), **1** in DMF (blue), SWCNT in DMF without **1** (red) and NH_2-PEO_{68}-NH_2 in DMF (pink); b) Images of SWCNT in DMF with/without **1**.

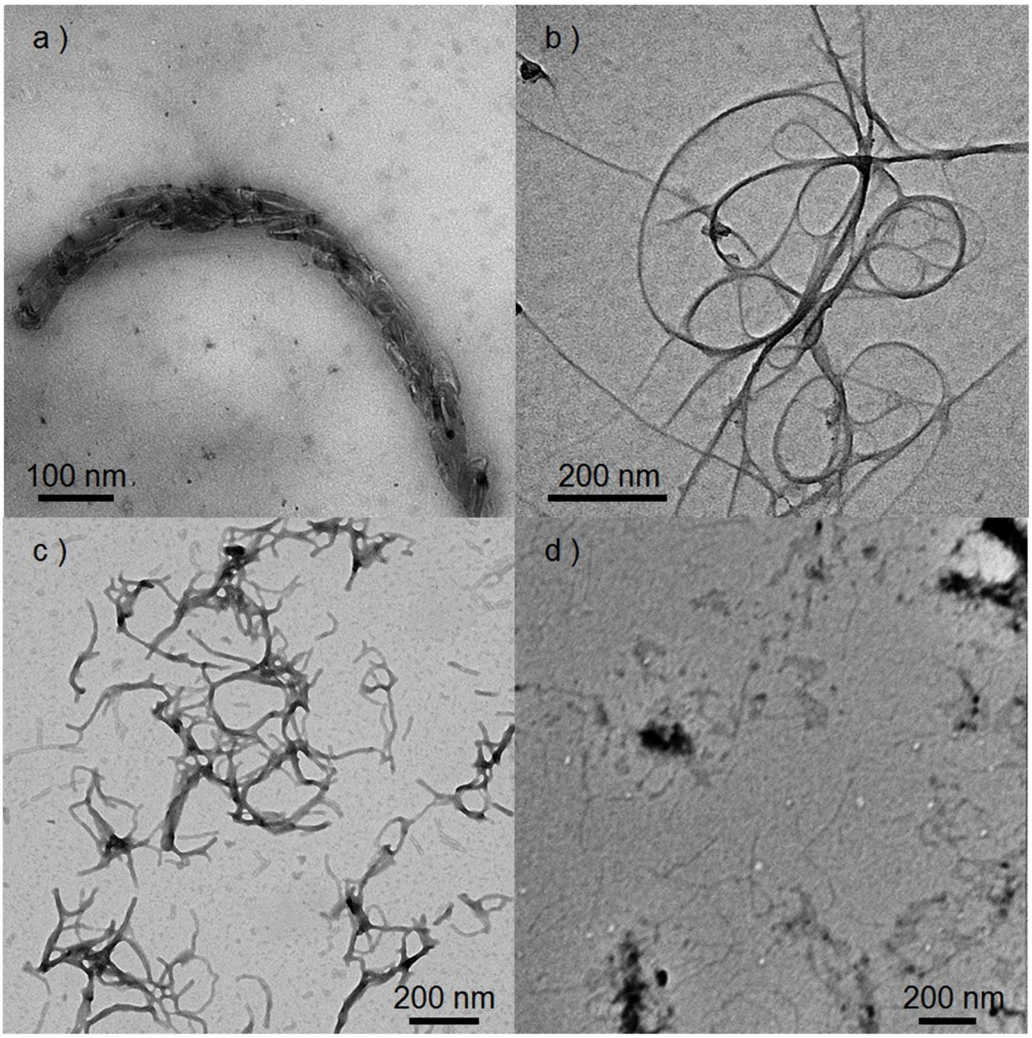

Figure 2.

TEM images of a) hierarchical assembly of **1**-SWCNT composites in SWCNT organogel without staining; b) SWCNT; c) **1** DMF organogel with PTA stain; d) **1** DMF organogel without staining.

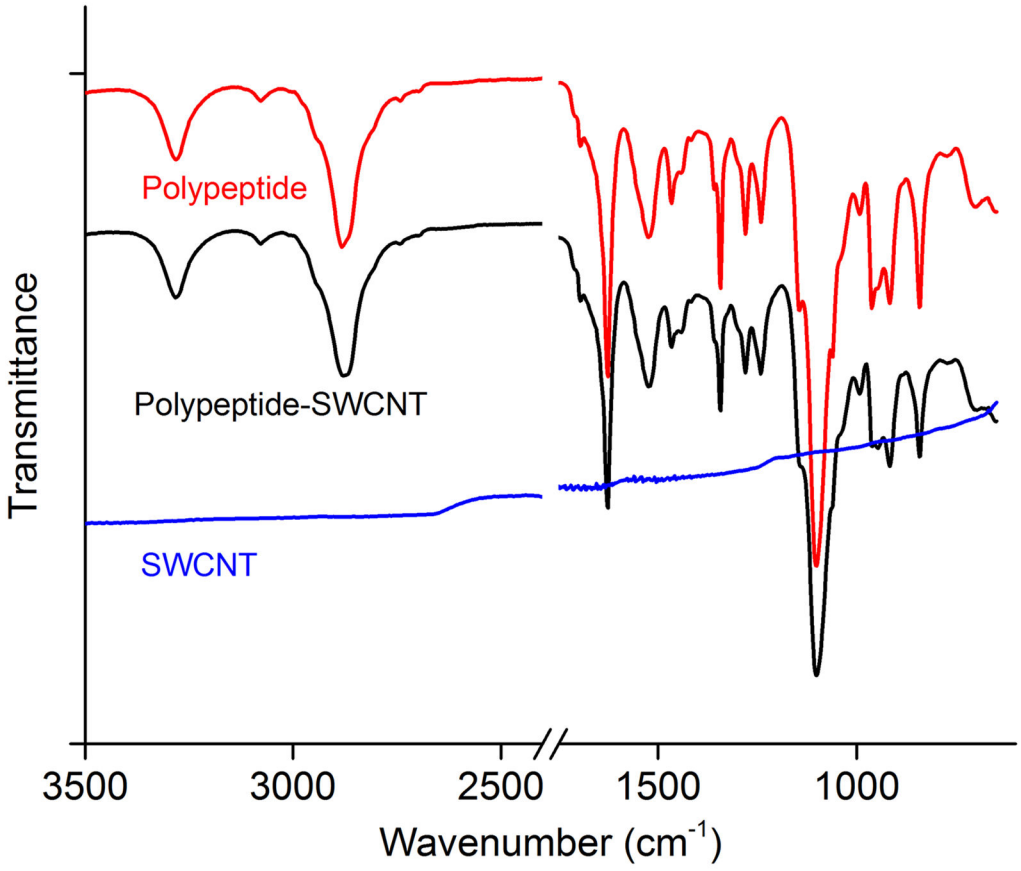

Figure 3.
FT-IR spectra of dried **1**, **1**-SWCNT composites and SWCNT.

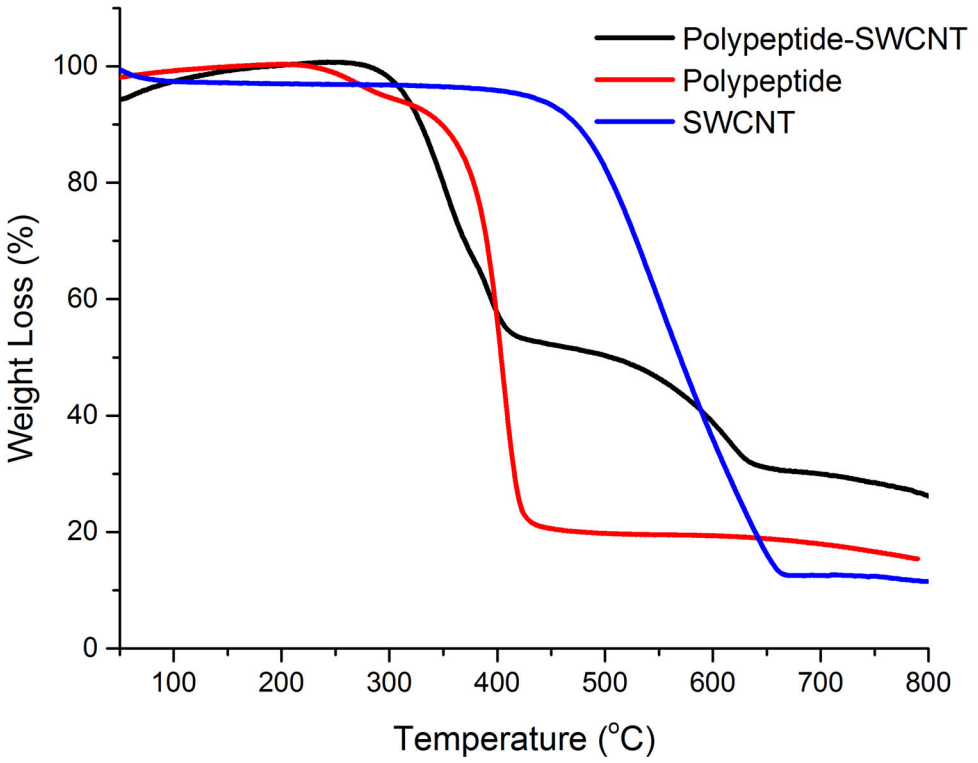

Figure 4.
TGA measurements of dried **1**, **1**-SWCNT composites and SWCNT.

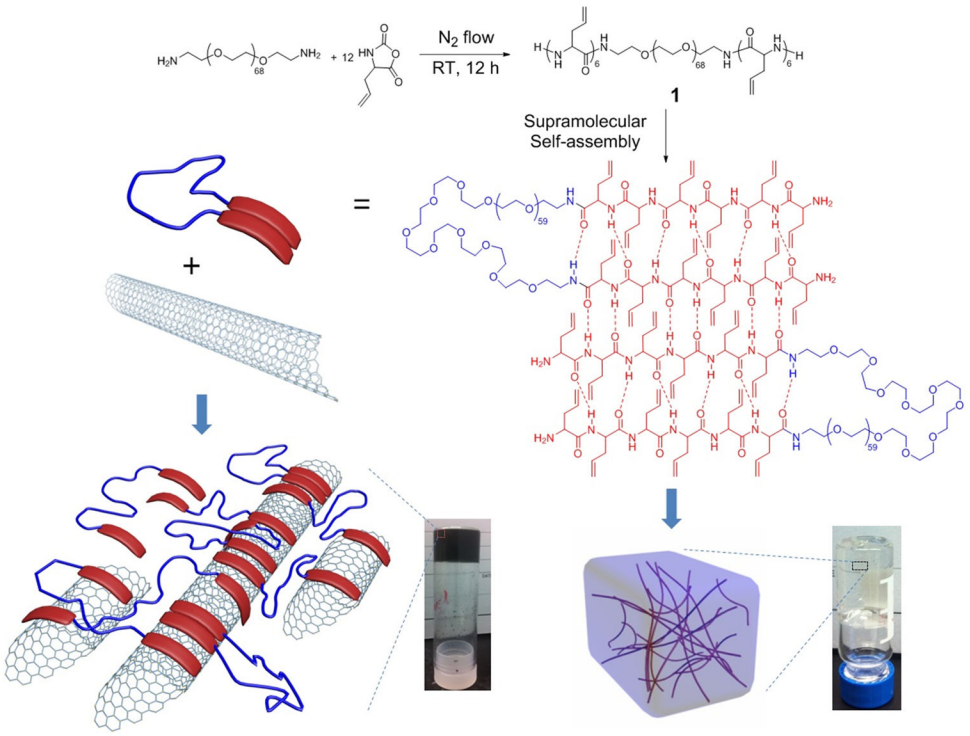

Scheme 1.

Graphic illustration of ODLAG$_6$-*b*-PEO$_{68}$-*b*-ODLAG$_6$ based organogels with/without SWCNT incorporation.